Korean J. Chem. Eng., **31**(6), 1028-1035 (2014)
DOI: 10.1007/s11814-013-0287-1

pISSN: 0256-1115
eISSN: 1975-7220

Synthesis, recognition and evaluation of molecularly imprinted polymer nanoparticle using miniemulsion polymerization for controlled release and analysis of risperidone in human plasma samples

Ebadullah Asadi*, Saman Azodi-Deilami*, Majid Abdouss*,†, Davood Kordestani, Alireza Rahimi***, and Somayeh Asadi******

*Department of Chemistry, Amirkabir University of Technology, P. O. Box 15875-4413, Tehran, Iran
**Faculty of Chemistry, Department of Organic Chemistry, Razi University, Kermanshah, Iran
***Electrochemistry and Inhibitors Group, Environmental Protection Department,
Research Institute of Petroleum Industry (RIPI), West Blvd of Azadi Sport Complex, Tehran, Iran
****Student Research Committee, Kermanshah University of Medical Sciences, Kermanshah, Iran
(*Received 10 August 2013 • accepted 19 December 2013*)

Abstract−We prepared high selective imprinted nanoparticle polymers by a miniemulsion polymerization technique, using risperidone as the template, MAA as the functional monomers, and TRIM as the cross-linker in acetonitrile as solvent. The morphology of the nanoparticles determined by scanning electron microscopy (SEM) images and drug release, binding properties and dynamic light scattering (DLS) of molecularly imprinted polymers (MIPs) were studied. Controlled release of risperidone from nanoparticles was investigated through in 1% wt sodium dodecyl sulfate aqueous solution and by measuring the absorbance by HPLC-UV. The results showed that the imprinted nanoparticles exhibited a higher binding level and slower release rate than non-imprinted nanoparticles, which contributed to interaction of risperidone with imprinted cavities within nanoparticles. Furthermore, the results from HPLC showed good precision (5% for 50.0 μg L^{-1}) and recoveries (between 86-91) using MIP from human plasma samples.

Keywords: Molecularly Imprinted Polymers, Risperidone, Sustained Release, Human Plasma, Miniemulsion Polymerization

INTRODUCTION

In nature, molecular recognition plays a decisive role in biological activity, for example in receptors, enzymes and antibodies. Utilizing this biochemical machinery as a model for variety of applications, scientists have been working to mimic the molecular recognition of biological molecules. Molecular imprinting is a technique whereby selective recognition sites can be created in synthetic polymers. This is achieved by forming a highly cross-linked polymeric matrix between functional monomers and a target compound (template) [1-3]. There are three approaches to molecular imprinting: covalent, non-covalent and semi-covalent. Application of non-covalent approach is the broadest among the three, because it is much more flexible and facile than the covalent or semi covalent approach [4]. The approach relies on the formation of a pre-polymerization complex between monomers carrying suitable functional groups and the template. The interaction between functional monomers and template during polymerization is complementary of the binding sites between polymer and the template; a host-guest relationship is produced. As a result, the non-covalent approach is the one most frequently used for imprinting, as it is open to a wide range of templates. In addition to the simple processes used to extract the template a greater number of higher affinity sites are generated. Molecularly imprinted polymer (MIP) is a synthetic polymer possessing selective molecular recognition properties because of recognition sites within the polymer matrix that are complementary to the analyte molecule in the size, shape and positioning of functional groups [2]. The selective recognition property in addition to the robustness and ease of preparation of MIPs has made them attractive for wide application such as in drug delivery systems [5-9], competitive drug assays [10], chemical sensing [11], solid phase extraction [12], chemical catalysis [13], chiral separation [14] and enantioseparation [15, 16]. The discovery of novel phenomena and processes into the nanoscale has created great excitement in biomedical research and technologies that can provide numerous novel biomaterials such as nanoparticles with appropriate dimension utilized potentially as drug-carriers for drug delivery technologies. In addition, nanotechnology can be employed to produce MIPs which may be used as important recognition materials in the construction of drug delivery systems (DDS). The improvement of MIP synthesis to obtain MIP nanoparticles could provide more potential use in biotechnology because the binding sites should be at or near the surface, giving good accessibility and selectivity [17-21].

This field of study has been receiving wide recognition and research interest over the years. Today, MIP is routinely synthesized in many laboratories by using traditional bulk imprinting methodology. With its ease and low-cost production of antibody mimicry that is robust and reusable, the technique has realized the long-time dream of many. However, the inherent limitations associated with the conventional approach of molecular imprinting simply means that more research effort will be necessary. First, with traditional molecular imprinting, bulky imprinted polymer is obtained where

†To whom correspondence should be addressed.
E-mail: phdabdouss44@aut.ac.ir

post-treatments like grinding and sieving are required. This gives rise to significant material wastage and produces irregular, sharp-edged polymeric bits where their applications in certain areas will be restrained. Additionally, with the creation of imprinted cavities within the polymer bulk, limited diffusion is often encountered for the removal and rebinding of template molecules [22,23]. This is especially important for the imprinting of macromolecules like proteins and oligosaccharides [24,25]. We employed miniemulsion polymerization as the primary imprinting polymerization system for the preparation of surface imprinted polymeric beads. Miniemulsion polymerization is a polymerization technique that can routinely produce monodispersed particles of sizes between 50-500 nm. The strong propensity of water-soluble protein molecules to be bound and adsorbed to the water-oil phase boundary formed by the surfactant micelles is made use of to prepare surface-imprinted polymeric nanoparticles. We also hypothesized that imprinted particles with sizes in the nano-range would provide large surface area for template molecular uptake. Most of all, with excellent heat transfer property, miniemulsion polymerization is extremely suitable for industrial application.

Risperidone,3-[2-[4-(6-fluoro-1,2-benzisoxazol-3-yl)-1-piperidinyl] ethyl]-6,7,8,9-tetrahydro-2-methyl-4H-pyrido[1,2-*a*] pyrimidin-4-one is an approved antipsychotic drug belonging to the chemical class of benzisoxazole derivatives and is available as tablet, oral liquid (Risperidal®) and orally disintegrating tablet (Risperidal® M-TAB). These dosage forms exhibit low bioavailability due to extensive first pass metabolism and non-targeted delivery results in numerous side effects. Since the target site of the risperidone is the brain, a strategy is desirable that not only improves the bioavailability by preventing first pass metabolism but also provides targeting to the receptor site and bypasses the blood-brain barrier, so as to achieve desired drug concentration at the site of action, hence preventing availability of drug at non-targeting sites and reducing the side effects.

The availability of polymer systems that can bind selectivity to a target molecule, release a host of new technologies and allow the controlled-release of a drug makes the drug delivery systems (DDS) application of molecularly imprinted polymers (MIPs) more attractive [26-30]. The potential advantage of imprinted polymers capable of DDS is the longer presence of the drug within the body. This paper focuses on using miniemulsion polymerization to prepare molecularly imprinted nanoparticles and capability of MIPs for controlled release of risperidone.

MATERIALS

Methacrylic acid (MAA) from Merck (Darmstadt, Germany), distilled under reduced pressure prior to use. Trimethylolpropane trimethacrylate (TRIM) and 2,2-azobis isobutyronitrile (AIBN) were purchased from Sigma-Aldrich (Steinheim, Germany). AIBN was recrystallized from methanol prior to use. Sodium dodecyl sulfate (SDS) and hexadecane (Merck, Hohenbrunn, Germany) were used without further purification. Risperidone (RSP) was obtained from the Ministry of Health and Medical Education (Tehran, Iran). Dialysis tubes (Sigma dialyses tubes Mw cutoff 12 kDa) were heated in an aqueous solution of 2% wt sodium hydrogen carbonate and 0.05% wt ethylene diamine tetra acetic acid (EDTA) and then kept under refrigeration in an aqueous solution of 0.05 wt sodium azide until use. Other reagents and solvents were of analytical grade.

Table 1. Polymer compositions and the percentage of RSP bound by each matrix

Polymer	Template : Monomer	RSP (mmol)	MAA (mmol)	TRIM (mmol)	Retention (%)[a]
MIP_1	1 : 2	2	4	16	55 (±1.4)
MIP_2	1 : 4	1	4	16	75 (±1.0)
MIP_3	1 : 6	0.5	4	16	59 (±1.2)
MIP_4	1 : 8	0.25	4	16	47 (±1.7)
NMIP	-	-	4	16	4 (±1.5)

[a]Average of three determinations

1. Procedures for Preparation of RSP-imprinted Polymeric Nanoparticles

Nanoparticles were prepared using miniemulsion polymerization from mixtures of the composition shown in Table 1. Briefly, the cross linker (TRIM), functional monomer (MAA), and hydrophobic agent (hexadecane, 0.2 ml) were mixed. Then, the template (RSP) and initiator (AIBN, 0.3 mmol) were added to the mixture. The mixture obtained was sonicated in an ultrasonic bath (SONO SWISS SW 12 H) for 20 min to ensure that all material was dissolved. The solution was gently mixed for 30 min until a hydrogen interaction between MAA and RSP occurred. This solution of organic phase was slowly poured through a syringe equipped with a 20-G angiocatheter into 30 ml water containing 45 mg dissolved SDS using a high-speed homogenizer (IKA, T25, Ultra-Turrax, USA) at 24,000 rpm for 4 min. The prepared emulsion was sonicated for 2 min and deoxygenated with dry nitrogen for 5 min. The polymerization was carried out in a three-necked glass reactor equipped with a mechanical stirrer and a nitrogen gas inlet to maintain a nitrogen atmosphere. The reactor was immersed in a water bath with thermostatic control to maintain the desired temperature at 70±1 °C for 16 h. The obtained nanoparticles were then collected by centrifuging (Sigma 3K30, Germany) at 17,000 rpm for 30 min. Nanoparticles were purified out by subsequent dialyses against 1 *l* deionized water (four times for 3 h). The produced nanoparticles were then centrifuged and dried in an oven (Memmert UNB 400, Germany) at 50 °C overnight. The template of non-leached imprinted polymers was removed by batch-mode solvent extraction with 40 mL of methanol containing 10% acetic acid (v/v) five times for 1 h, until no template could be detected from the washing solvent by HPLC-UV at a wavelength of 240 nm. The nanoparticles were finally washed with deionized water and acetone, and the resulting leached imprinted nanoparticles was dried at 50 °C overnight. Non-imprinted polymers (NMIPs) were synthesized under identical conditions without the template.

As Table 1 shows, different ratios of monomers MAA to the template were used in the experiment. The optimal ratio of the functional monomers to the template for RSP by miniemulsion polymerization was 4 : 1, which had the best specific affinity and the highest retention of 75%, while that of the corresponding NMIP was 4%. Excess of the functional monomer with respect to the template yielded higher non-specific affinity. Therefore, the typical 1 : 4 : 16 (template: monomer: cross linker mole) ratio was used for further studies.

2. Differential Scanning Calorimetry (DSC)

The thermal properties of polymer particles and RSP were inves-

tigated using a Mettler DSC 823 (Mettler Toledo, GmbH, Switzerland) equipped with a Julabo thermocryostate model FT100Y (Julabo Labortechnik GmbH, Germany). A Mettler Star software system (version 9.x), used for data acquisition and indium, was used to calibrate the instrument. The samples were heated at a speed of 10 °C min^{-1} up to 450 °C.

3. Morphologic Analysis

Scanning electron microscopy (SEM, PhilipsXL30 Scanning Microscope, Philips, Netherlands) was employed to determine the shape and surface morphology of the produced polymer particles. The polymer particles were sputter coated with gold prior to the SEM measurement. The particle size and size distribution of polymer particles were measured by dynamic light scattering (DLS, Malvern Zetasizer ZS, Malvern, UK). The polymer particles were measured at a fixed scattering angle of 90°.

Pore size distribution and specific surface area analysis of polymer particles were done by nitrogen adsorption-desorption using a BELSORPMini II (Japan) at 196 °C. Prior to measurement, 150 mg of the polymer particles was heated at 100 °C for 2 h under vacuum. The specific surface area, pore volume and average pore diameter of polymer particles were obtained by Brunauer-Emmett-Teller (BET) method using BELSORP analysis software.

4. Chromatographic Conditions

The HPLC system consisted a Waters 515 pump, a 486Waters UV/Vis detector, *a model 7725i Rehodyne* injector with a 25 μL sample loop, and a micro-Bondapak *C18 column* of 4.6 mm×150 mm HPLC column. HPLC data was acquired and processed using a PC and Millennium 2010 Chromatogram Manager software (Version 2.1 Waters). The HPLC was carried out at room temperature. A degassed mixture of acetonitrile : phosphate buffer (0.01 mol L^{-1}, pH 3.0) (30 : 70) at a flow rate of 1.1 ml min^{-1} was selected as a mobile phase [31]. All of the analyses were recorded by *Millennium chromatography* software.

5. Binding Experiment

For measuring of template binding, 50 mg of polymer nanoparticles was added to 10 ml RSP solution (pH 7.0) of various initial concentrations in a conical centrifugation tube and sealed. The mixtures were thermostated at 25 °C for 24 h under continuous stirring and then filtrated on paper filter. Then, the residual concentration of RSP in solution was established using HPLC-UV at 240 nm. The quantity (Q) of the template bound to MIP or NMIP was calculated according to the following equation [32]:

$$Q=[(C_0-C_t)\times V]/W$$

where C_0 and C_t (mg/L) are the initial concentration and the residual concentration of RSP, respectively; V (L) is the initial volume of the solution, and W (g) is the weight of the MIPs or NMIPs.

6. Drug Loading through Soaking Procedure

Fifty mg of polymers was suspended in 10 mL of RSP solution (0.05 mM) and soaked for 30 min at room temperature. During this time, the mixture was continuously stirred and then the solvent was removed. Subsequently the MIP particles were dried under vacuum overnight at 40 °C.

7. Drug Release Experiments

Release studies from RSP loaded nanoparticles were carried out in appropriate solution of RSP in SDS solution (1% wt) as a medium used to provide sink conditions. Fifty mg of nanoparticles was incubated in 16 ml of 0.05 mM RSP water/acetonitrile (1 : 4, v/v) solution for 60 min. Unbound RSP was removed from the nanoparticles by centrifugation at 20,000 rpm for 30 min. Afterwards, the centrifuged nanoparticles suspended in 5 ml of the SDS solution (1% wt) and placed in a dialysis tube sealed at both ends with medicell clips, and soaked in 45 ml of the SDS solution (1% wt). The medium was stirred at 100 rpm. Aliquots of 3 ml were withdrawn from the medium at designed time intervals. An equivalent volume of the SDS (1% wt) aqueous solution was added to maintain the volume of the medium at 45 ml. The amount of RSP released from each nanoparticle was determined during time-resolved release studies quantified by HPLC-UV analysis.

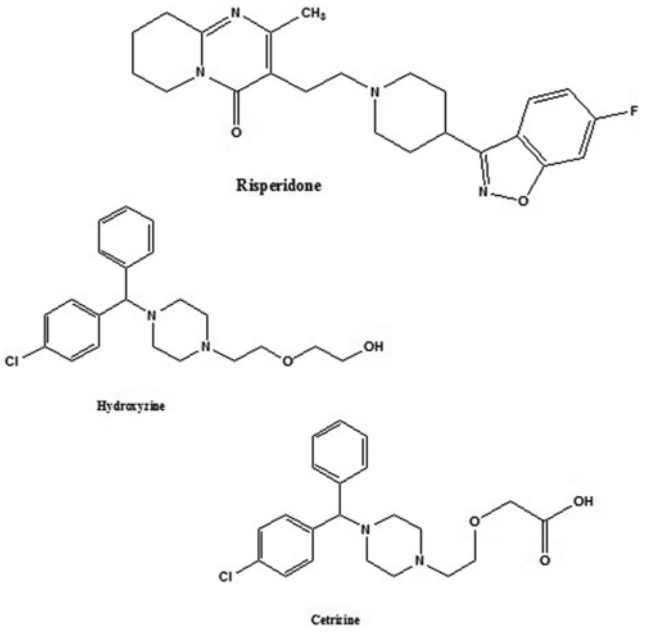

Fig. 1. Chemical structures of investigated drugs.

8. Extraction Procedure for Human Plasma Samples

Drug-free human plasma was obtained from the Iranian blood transfusion service (Tehran, Iran) and stored at −20 °C until use after gentle thawing. Due to possibility of protein-bonding for risperidone and reducing the recoveries processes, it was necessary to have some treatments with plasma before extraction with MMIP particles. So, the plasma samples was diluted with 25 mM ammonium acetate (pH 5.0), then centrifuged 30 min at 6,000 rpm to remove excess of proteins. Then the supernatant was filtered through a cellulose acetate filter (0.2 μm pore size, Advantec MFS Inc., CA, USA). The filtrate was collected in glass containers and stored at −20 °C until the analysis was performed. Two mL of the filtered supernatant was collected to be directly percolated through the MMIP or the MNIP.

RESULTS AND DISCUSSION

1. Thermal Analysis

DSC studies performed to investigate the thermal characteristics of the nanoparticles. Fig. 2 shows the DSC thermograms of pure RSP, non-imprinted nanoparticles, and leached and non-leached imprinted nanoparticles. Pure RSP exhibited an endothermic peak

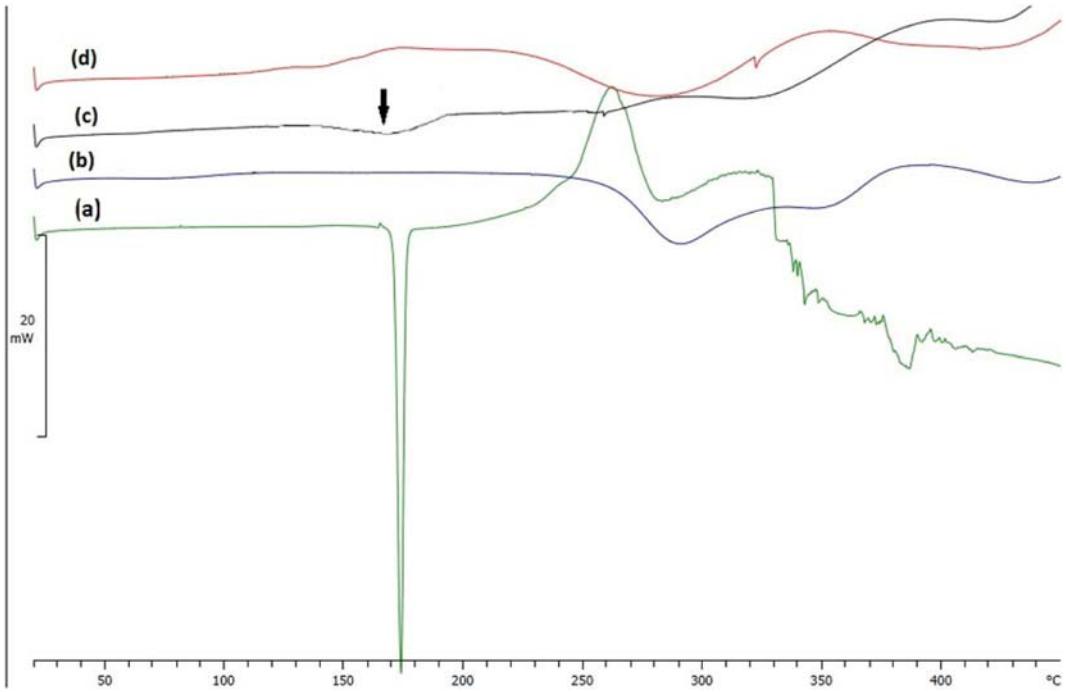

Fig. 2. RSP (a), leached MIP_2 (b), non-leached MIP_2 (c) and NMIP (d).

of the melting point at about 175 °C. DSC results showed that all imprinted and non-imprinted polymers were thermally stable up to approximately 300 °C. This good thermal stability was due to the high level of cross-linking of the prepared polymers, which is favorable for different applications. All polymers showed similar thermal behavior, but a transition was observed at 175 °C in the thermograms of non-leached imprinted nanoparticles that contained RSP, which could be explained as the melting point of RSP.

2. Study of Morphology and Porosity of Nanoparticles

The morphology of the MIP_2 particles, determined by a scan-

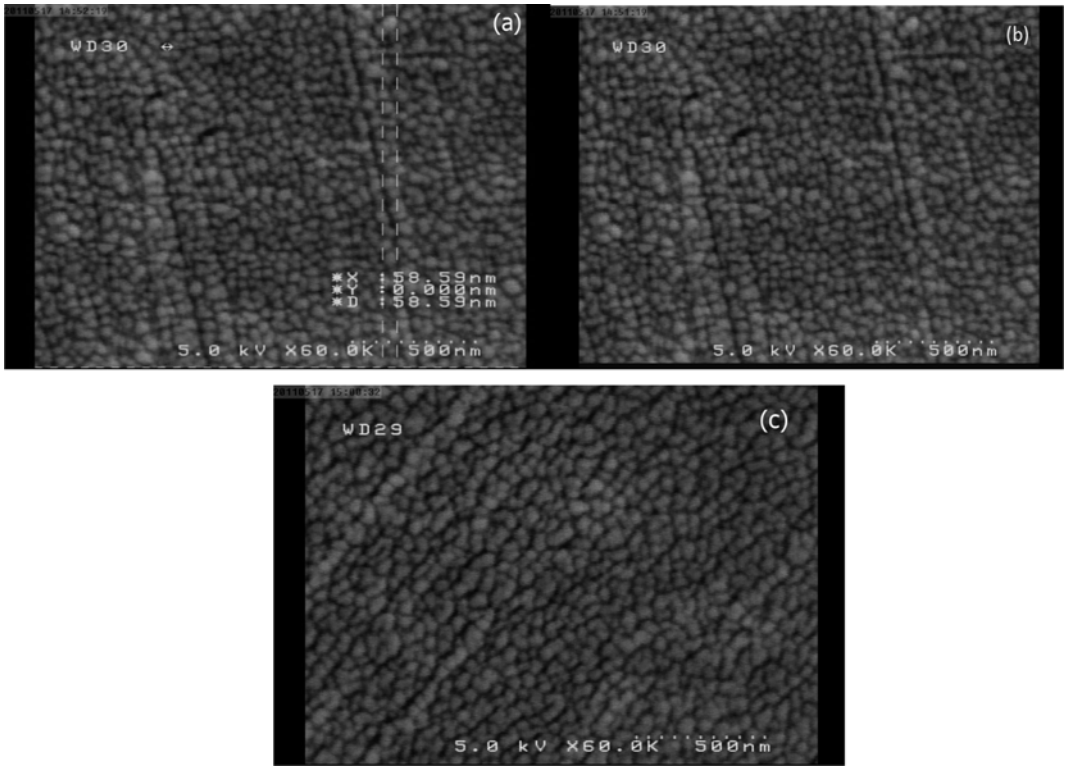

Fig. 3. Scanning electron micrographs, leached MIP_2 (a), non-leached MIP_2 (b), NMIP (c).

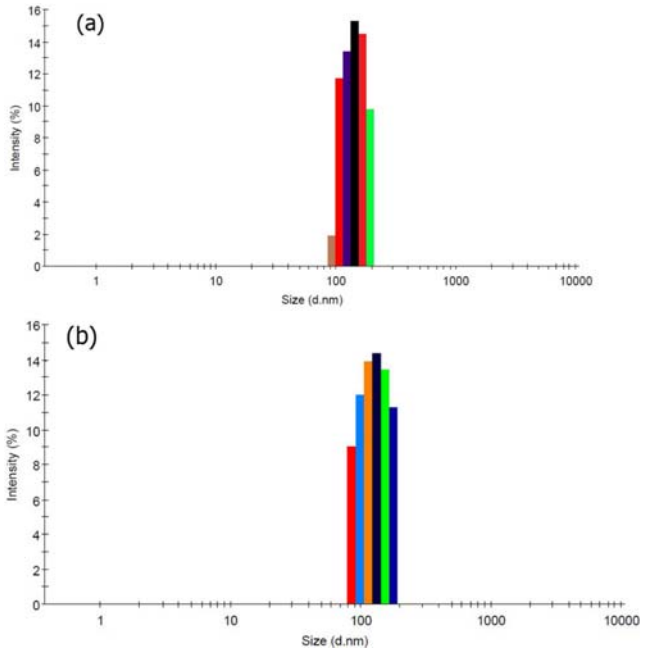

Fig. 4. Particle size distribution of MIP_2 (a) and NMIP (b) measured by dynamic light scattering.

ning electron microscope (SEM), is shown in Fig. 3, with MIP_2 and NMIP particles at a magnification of 500-1,000 nm.

Particle size measurements were performed by dynamic light scattering (DLS) analysis. Fig. 4 shows a very narrow particle size distribution for nanoparticles. The polydispersity index (PdI) and Z-Average for MIPs were 0.124 and 182.6 and for NMIPs were 0.082 and 167, respectively. The monodispersed size for nanoparticles is desirable in many applications, such as electrocatalysts [33], solid-phase micro extraction (SPME) [34], and development of sensors using microsphere deposition [35], capillary electrochromatography [36], and drug delivery systems [37].

The specific surface area, pore volume and average pore diameter of polymer particles were obtained by Brunauer-Emmett-Teller (BET) method using BELSORP analysis software. Most solids of high surface area are to some extent porous. The texture of such materials is defined by the detailed geometry of the void and pore space. Porosity, ε, is related to texture and refers to the pore space in a material. An open pore is a cavity or channel communicating with the surface of a particle, as opposed to a closed pore. The void is the space or interstice between particles. In the context of extraction and fluid penetration, powder porosity is the ratio of the volume of voids plus the volume of open pores to the total volume occupied by the powder. Similarly, particle porosity is the ratio of the volume

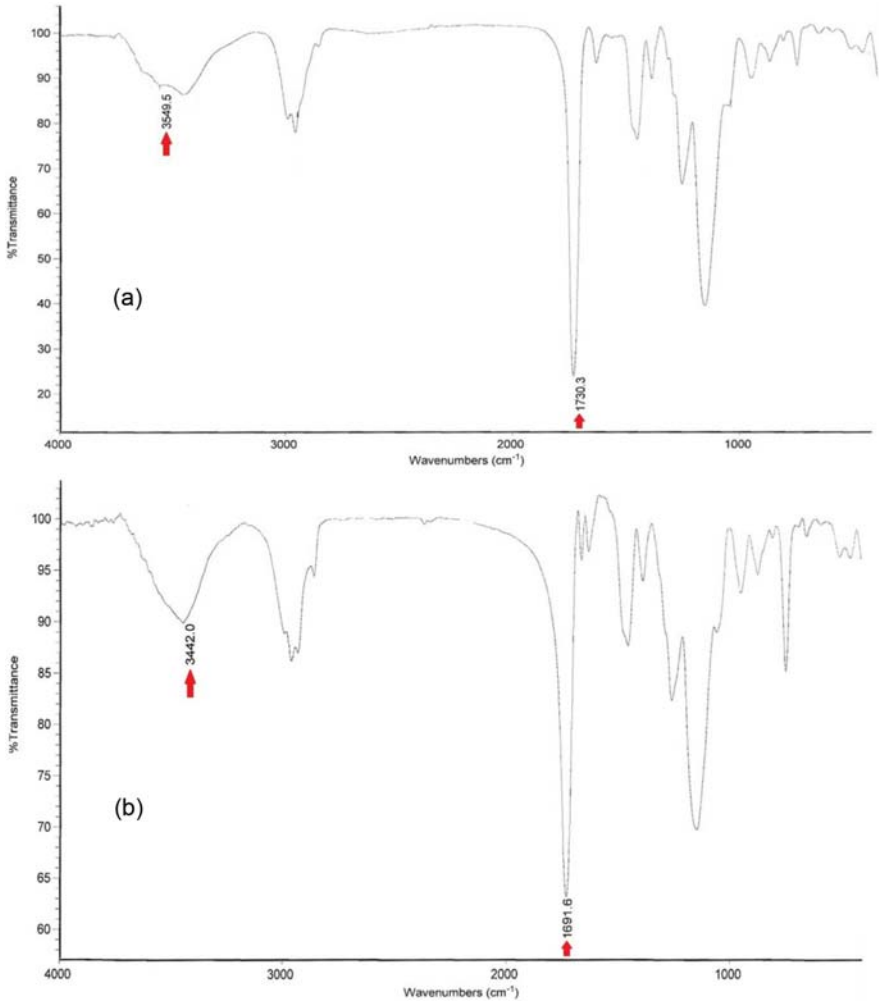

Fig. 5. Infrared plots of the leached (a) and non-leached (b) MIP particles.

of open pores to the total volume of the particle. Note that these definitions place the emphasis on the accessibility of pore space to the adsorptive. The extraction isotherm obtained has been analyzed using BET equation and BJH algorithm, the obtained results for specific surface area (m^2/gr), specific pore volume (cm^3/gr) were 255 and 1.19, respectively.

3. Characterization

The FT-IR spectra of the ground polymers were recorded (EQUINOX 55, Bruker). The spectra of NMIP and the non-leached and leached MIP_2 displayed similar characteristic peaks, indicating a similarity in the backbone structure of the different polymers. The IR spectra of the non-leached and leached nano imprinted poly (MAA *co*-TRIM) are shown in Fig. 5. As a result of the hydrogen binding with the -COOH group of MAA, the C=O stretching, the OH stretching, and the bending vibrations at 1,691.6, 3,442, and 1,392.6 cm^{-1} in the non-leached MIP_2 materials were shifted to 1,730.3, 3,549.5, and 1,391.3 cm^{-1} in the corresponding leached MIP_2, respectively. Other absorption peaks match those of MIP_2, as well as NMIP: 1,250, 1,125 cm^{-1} (symmetric and asymmetric ester C-O stretch bands), 1,641 cm^{-1} (stretching vibration of residual vinylic C=C bonds), and 960 cm^{-1} (out-of-plane bending vibration of vinylic C-H bond).

TGA (Perkin Elmer TGS-2) was performed at the maximum heating rate of 20 °C min^{-1} in an oxygen atmosphere. Regarding the non-leached MIP particles, TGA revealed two decomposition states: one mass loss at 100 °C (10% weight loss), assigned to the decomposition of the free monomer and the cross-linker, and one starting at 175 °C, related to the RSP decomposition as the melting point of RSP is 175 °C. All the materials were completely decomposed prior to reaching 460 °C. These observations indicated that the rigidity of the non-leached and leached MIP_2 particles is more than blank materials, as the former exhibit decomposition above ~300 °C; the latter starts its decomposition at ~250 °C onwards. Also, the non-leached and leached MIP particles have similar degradation patterns above 400 °C. The complete decomposition of the polymeric matrix occurs for both at temperatures above 450 °C.

4. Effect of pH on Drug Loading

The effect of pH on the sorption of RSP was examined by varying the pH of solutions from 3.0 to 12.0. Several batch experiments were performed by equilibrating 50 mg of the imprinted particles with 5 mL of the solutions containing 0.05 mM of RSP under the desired levels of pH. The results for different polymers (Fig. 6) indicated that pH has great effect on loading. The percentage of RSP retention increases up to 7.0 pH and then it decreases by further increase of pH. A difference of about 71% between MIP_2 and NMIP was seen at the pH level of 7.0. Lesser effects were observed at lower and higher pH values and which may have been attributed to the protonation of the functional group of RSP and to deprotonation of carboxyl groups of the polymer, respectively.

5. Adsorption Capacity of Polymers

One of the important factors we studied was the capacity of a sorbent to quantitatively remove a specific amount of template from the solution. Once the system has come to equilibrium, the amount of free template in the solution is measured to determine the amount of adsorbed template. In the measurement of adsorption capacity of MIP and NMIP absorbents, 50 mg samples of the absorbents were added to 100 mL RSP solutions at concentrations of 10-500 μg ml^{-1}. The suspensions were mechanically shaken at room temperature, followed by centrifuging and removal of absorbents. The remaining RSP in the supernatant was measured by HPLC-UV. The adsorption isotherm, which is the number of milligrams adsorbed per gram of adsorbent (Q) versus the equilibrium concentration of RSP, is shown in Fig. 7. According to these results, the maximum amount of RSP that can be absorbed by MIP is 93 mg g^{-1} at pH 7.0. As all the accessible specific cavities of the MIP particles are saturated, the retention of the analyte is mainly due to non-specific interactions, which can be identical for MIP and NMIP polymers.

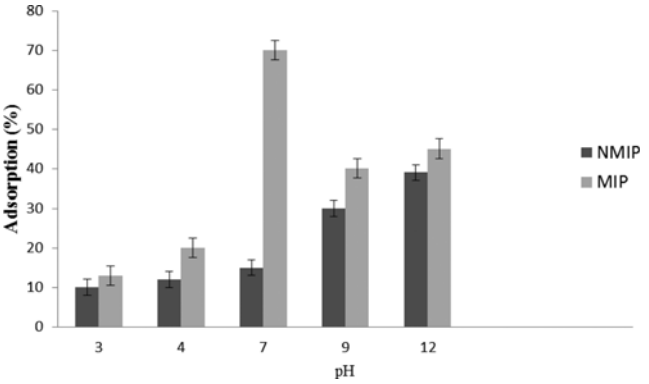

Fig. 6. Effect of pH on rebinding efficiency of risperidone. 50 mg of the imprinted polymers; sample volume: 5 mL; risperidone concentration: 0.05 mM; room temperature (mean± S.D., n=3).

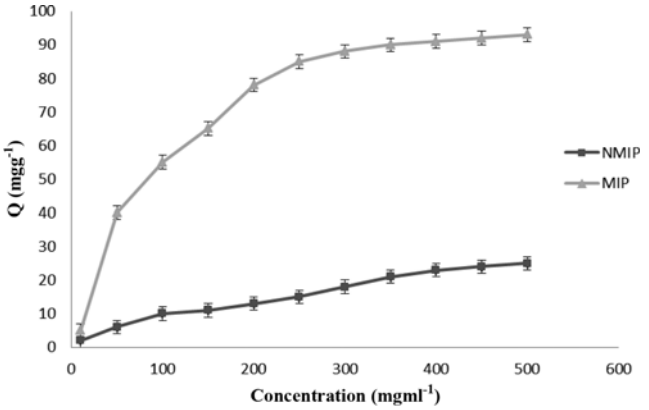

Fig. 7. Effect of RSP concentration on the adsorption capacity on MIP and NMIP nanoparticles at pH 7.0.

6. Study of MIP Selectivity

Chromatographic evaluation and equilibrium batch rebinding experiments are the methods most commonly used to investigate the selectivity of the imprinted materials [38]. For equilibrium batch rebinding experiments, a known mass of the template in solution is added to a vial containing a fixed mass of the polymer. Once the system has reached equilibrium, the concentration of the free template in solution is measured and the mass of the template absorbed to the MIP is calculated [39]. Risperidone, Hydroxyzine and Cetrizine were selected to investigate the selectivity of the nanoparticles MIP. Their molecular structures are shown in Fig. 1. Solutions of all the compounds were prepared individually with the concentration of 0.05 mM. The extraction of the solvent was 10% (v/v) AcOH/MeOH. The extraction yields of the selected compounds with the

Table 2. Adsorption of risperidone, hydroxyzine and cetrizine with MIP and NMIP at 50 mM concentration. V=5 ml; pH 7 at room temperature (mean±S.D., n=3)

Compounds	Adsorption (%)	
	MIP	NMIP
Risperidone	75±1.0	4±1.5
Hydroxyzine	20±1.2	12±1.3
Cetrizine	15±1.7	10±1.1

MIP and NMIP are shown in Table 2. The extraction yields of the analogues with the MIP were much higher than that of the NMIP. It was revealed that the RSP based-MIP possess better affinity to the template molecule. This affinity is mainly caused by the hydrogen bonding interaction between the functional groups possessed by all drugs and carboxylic groups in the MIP. A possible reason for the difference is that the extractions of drugs were relative to their structural similarity with the template molecule of MIP.

7. Sustained Release Studies

Fifty mg of MIP and NMIP nanoparticles was added to 16 ml of RSP solution at a concentration of 0.05 mM. The suspensions were mechanically shaken at room temperature, followed by centrifuging and removal of absorbents. The remaining RSP in the supernatant was measured by HPLC-UV. Then, RSP-loaded nanoparticles were dispersed in 5 ml of 1% wt sodium dodecyl sulfate (SDS) aqueous solution and placed into a dialysis bag. The dialysis bag was placed in a flask containing 45 ml of release medium (1% wt SDS). The whole assembly was shaken at 100 rpm and room temperature. At predetermined time intervals, 3 ml of the release medium was removed and replaced with the fresh medium. The content of RSP in the medium was measured by HPLC-UV and the cumulative release percentage of RSP was calculated. The result of the release profile of RSP from nanoparticles is shown in Fig. 8. The initial quick release of RSP could be probably due to weakly adsorbed RSP molecules at the surface of the nanoparticles. Note that NMIP Nanoparticles released a considerable amount of RSP within 45 hours (about 95% of the RSP). Subsequently, the release of RSP from MIP nanoparticles was slower and was delayed up to 300 h with 100% of drug release. There was a comparable difference in release kinetics between different nanoparticles under these conditions. The release profiles of the imprinted nanoparticles were slower than that of the non-imprinted nanoparticles. This significant difference in the release of imprinted nanoparticles and NMIP could be attributed to the existence of specific sites in imprinted nanoparticles that had a strong interaction with RSP molecules.

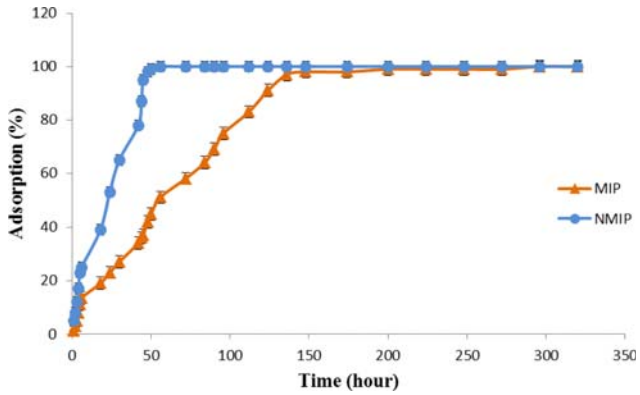

Fig. 8. In vitro drug release profile of 50 mg RSP imprinted nanoparticles at room temperature (mean±S.D., n=3).

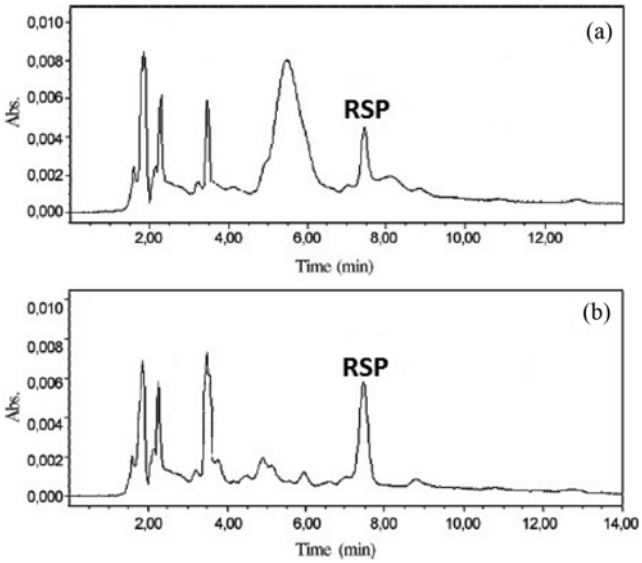

Fig. 9. HPLC chromatograms obtained after percolation of 2 mL human serum spiked with 50.0 μgL^{-1} of risperidone with a cleanup step comprising the (a) NMIP and (b) MIP monitored at 239 nm; conditions: column ACE 5 μm, C18 4.6 mm×250 mm at +40 °C, eluent acetonitrile: phosphate buffer (0.01 mol L^{-1}, pH 3.0) 40 : 60 at flow rate of 1.1 mLmin^{-1}.

8. Real Sample Analysis

To demonstrate the potential of MIP for the sample clean-up, the MIP was applied to the purification of spiked risperidone (RSP) in human plasma. Aqueous media was employed for the loading solution, and the wash procedure was assessed for obtaining maximum recovery of the analytes using acetone. The chromatograms obtained for plasma samples are shown in Fig. 9. This efficient method allowed cleaner extracts to be obtained and interfering peaks arising from the complex biological matrices to be suppressed. Results from the HPLC analyses in Table 3 show that the MIP extraction of RSP for plasma samples has good precision (5% for 50.0 μg L^{-1}) and recovery (between 86-91). Typical chromatograms (presented in Fig. 9) reveal that the MIP could be used for the sample clean up and when MIP sorbent was used, a board peak in chromatogram was omitted. The limit of detection (LOD) and limit of quantification (LOQ) for RSP in plasma samples were 0.2 and 0.5 μg L^{-1}.

Table 3. Assay of risperidone in human plasma

Sample	Spiked value (μg L^{-1})	Recovery%±SD[a]	
		MIP	NMIP
Human serum	5	86±1.0	14±1.2
	10	88±2.0	15±2.1
	25	87±1.6	16±1.3
	50	91±1.3	12±1.0

[a]Average of three determinations

The number of replicates for the experiment was three times.

CONCLUSION

We used novel synthetic conditions of miniemulsion polymerization to obtain nanosized RSP-molecularly imprinted polymers for application in the design of new drug delivery systems. The relationships between the morphology and porosity of particles, binding and release properties were detailed, providing useful guidelines for controlling the MIP particle properties for the desired application including analytical fields and drug delivery systems. The key factors controlling recognition and release by imprinted polymer matrices including mole ratios of monomer to RSP and medium nature and pH are discussed. In this case, the monomer/RSP ratio of 4 : 1 showed the best specific affinity of 75% and because of the existence specific binding sites, we obtained proper release profiles compared with the controlled polymers. The MIP nanoparticles revealed excellent binding properties at equilibrium binding conditions and can be used for specific capturing of template from dilute solutions. SDS solution (1% wt) as a medium was used to provide release studies from RSP loaded nanoparticles. The results showed the ability of MIP polymers to control RSP release, supporting a release mechanism in which the release rate of the drug from the matrices depends on the selective interaction between drug and imprinted cavities. For this reason, the rate of the release was considerably different, and MIP represents a very promising polymeric device for the selective and controlled release of RSP related to non-imprinted polymer. Moreover, the recoveries for the spiked human plasma samples were between 86-91% in 5-50 μgL^{-1} respectively. It could be concluded that the technique has great potential in developing selective extraction method for other compounds.

REFERENCES

1. K. Mosbach, *Trends Biochem. Sci.*, **19**, 9 (1994).
2. M. Esfandyari-Manesh, M. Javanbakht, F. Atyabi and R. Dinarvand, *J. Appl. Polym. Sci.*, **121**, 1118 (2011).
3. S. Tokonami, H. Shiigi and T. Nagaoka, *Anal. Chim. Acta*, **641**, 7 (2009).
4. G L. Yang, J. F. Yin and Z. W. Li, *Chromatographia*, **59**, 705 (2004).
5. K. C. Ho, W. M. Yeh, T. S. Tung and J. Y. Liao, *J. Anal. Chim. Acta*, **542**, 90 (2005).
6. S. Azodi-Deilami, M. Abdouss and S. R. Seyedi, *Cent. Eur. J. Chem.*, **8**, 687 (2010).
7. S. Azodi-Deilami, M. Abdouss and M. Javanbakht, *Appl. Biochem. Biotechnol.*, **164**, 133 (2011).
8. M. Abdouss, E. Asadi, S. Azodi-Deilami, N. Beik-mohammadi and S. Amir Aslanzadeh, *J. Mater. Sci. Mater. Med.*, **22**, 2273 (2011).
9. S. Azodi-Deilami, M. Abdouss and A. R. Hasani, *Cent. Eur. J. Chem.*, **8**, 861 (2010).
10. M. Javanbakht, S. Eynollahi Fard, A. Mohammadi, M. Abdouss, M. R. Ganjali, P. Norouzi and L. Safaraliee, *Anal. Chim. Acta*, **612**, 65 (2008).
11. P. T. Vallano and V. T. Remcho, *J. Chromatogr. A*, **887**, 125 (2000).
12. A. Kamal, B. A. Kumar, M. Arifuddin and S. G. Dastidar, *Bioorg. Med. Chem.*, **11**, 5135 (2003).
13. F. Puoci, M. Curcio, G. Cirillo, F. Lemma, U. G. Spizzirri and N. Picci, *Food Chem.*, **106**, 836 (2008).
14. W. Chen, D. K. Han, K. D. Ahn and J. M. Kim, *Macromol. Res.*, **10**, 122 (2002).
15. R. Suedee, T. Srichana and G. Martin, *J. Controlled Release*, **66**, 135 (2000).
16. H. Sambe, K. Hoshina, R. Moadel, W. Wainer and J. Haginaka, *J. Chromatogr. A*, **1134**, 88 (2006).
17. R. Suedee, *Int. J. Pharm. Sci. Rev. Res.*, **20**, 235 (2013).
18. K. Rostamizadeh, M. Vahedpour and S. Bozorgi, *Int. J. Pharm.*, **424**, 67 (2012).
19. L. Li, X. He, L. Chen and Y. Zhang, *Chem. Asian J.*, **4**, 286 (2009).
20. X. Ding and P. A. Heiden, *Macromol. Mater. Eng.*, DOI:10.1 002/mame.201300160 (2013).
21. Z. Lin, Z. Xia, J. Zheng, D. Zheng. L. Zhang, H. Yang and G. Chen, *J. Mater. Chem.*, **22**, 17914 (2012).
22. H. Yan and K. H. Row, *Int. J. Mol. Sci.*, **7**, 155 (2006).
23. F. Puoci, G. Cirillo, M. Curcio, F. Iemma, O. L. Parisi, U. G. Spizzirri and N. Picci, *Molecularly imprinted polymers (PIMs) in biomedical applications*, Biopolymers, Magdy Elnashar (Ed.), InTech (2010).
24. C. J. Allender, C. Richardson, B. Woodhouse, C. M. Heard and K. R. Brain, *Int. J. Pharm.*, **195**, 39 (2000).
25. J. Y. Ju, C. S. Shin, M. J. Whitcombe and E. N. Vulfson, *Biotechnol. Bioeng.*, **64**, 232 (1999).
26. C. Alvarez-Lorenzo and A. Concheiro, *Biotech. Ann. Rev.*, **12**, 225 (2006).
27. H. Hiratani and C. Alvarez-Lorenzo, *J. Controlled Release*, **83**, 223 (2002).
28. C. Alvarez-Lorenzo and A. Concheiro, *J. Chromatogr., B*, **804**, 231 (2004).
29. C. Alvarez-Lorenzo, F. Yanez, R. Barreiro-Iglesias and A. Concheiro, *J. Controlled Release*, **113**, 236 (2006).
30. B. Sellergren and C. J. Allender, *Adv. Drug Deliv. Rev.*, **57**, 1733 (2005).
31. M. Turchan, P. Jara-Ulloa, S. Bollo, L. J. Nunez-Vergara, J. A. Squella and A. Alvarez-Lueje, *Talanta*, **73**, 913 (2007).
32. J. Jiang, K. Song, Z. Chen, Q. Zhou, Y. Tang, F. Gu, X. Zou and Z. Xu, *J. Chromatogr. A*, **1218**, 3763 (2011).
33. L. Jiang, G. Sun, Z. Zhou, S. Sun, Q. Wang, S. Yan, H. Li, J. Tian, J. Guo, B. Zhou and Q. Xin, *J. Phys. Chem. B*, **109**, 8774 (2005).
34. C. Huang and B. Hu, *Spectrochim. Acta B*, **63**, 437 (2008).
35. I. Aruna, F. E. Kruis, S. Kundu, M. Muhler, R. Theissmann and M. Spasova, *J. Appl. Phys.*, **105**, 064312 (2009).
36. C. Nilsson and S. Nilsson, *Electrophoresis*, **27**, 76 (2006).
37. M. Gaumet, A. Vargas, R. Gurny and F. Delie, *Eur. J. Pharm. Biopharm.*, **69**, 1 (2008).
38. P. Martin, G R. Jones, F. Stringer and I. D. Wilson, *Analyst.*, **128**, 345 (2003).
39. W. M. Mullet, M. Walles, K. Levsen, J. Borlak and J. Pawliszyn, *J. Chromatogr. B.*, **801**, 297 (2004).